

Influence of zinc content on some properties of Ni–Zn ferrites

A.M. El-Sayed

Inorganic Chemistry Department, National Research Centre, Tahrir Street, Dokki, Cairo 12622, Egypt

Received 27 May 2001; received in revised form 6 June 2001; accepted 19 August 2001

Abstract

The chemical formula of the samples investigated is $\text{Ni}_{1-y}\text{Zn}_y\text{Fe}_2\text{O}_4$, where $y=0.1, 0.3, 0.5, 0.7$ and 0.9 . The specimens were prepared by the usual ceramic technology and sintered at 1250°C in static air atmosphere. The influence of Zn content on the densification and microstructure characteristics of specimens was studied. X-ray diffraction and IR absorption spectra were used for analysing the compositions. It was found that the samples have spinel cubic structure and sintered to about 97–98% of the corresponding X-ray density. Exaggerated grain growth with fine pores inside the grains were observed with increasing Zn content. The overall results are discussed in light of the existing understanding of these systems. © 2002 Elsevier Science Ltd and Techna S.r.l. All rights reserved.

Keywords: A. Sintering; B. Microstructure; Ni–Zn ferrites; Preparation

1. Introduction

Nickel–zinc ferrites can be classed as “good all-around performers” because they cover a range of applications from low frequency to microwave and from low to high permeability. These ferrites have been found to be one of the most versatile of the ferrite systems for general use. The polycrystalline ferrites are a complex system composed of crystallites, grain boundaries, and pores. The magnetic properties of these ferrites are determined by chemical composition, porosity, grain size, etc. [1]. The microstructure of the substituted nickel ferrite depends on the sintering condition and the deviation from stoichiometry as well as on the presence of flux component (CuO , Bi_2O_3 , V_2O_5) [2]. The chemical composition of a ferrite affects its properties. If the dependence of a physical property on the composition is known for a given mixed ferrite, then it is possible to obtain a ferrite possessing the desired physical property by choosing the appropriate composition at a particular temperature. With this in view a study of the dependence of some properties of nickel–zinc ferrites, sintered at 1250°C , on its compositions has been undertaken; the results are presented in this paper.

2. Experimental

Ferrite samples compositions: $\text{Ni}_{1-y}\text{Zn}_y\text{Fe}_2\text{O}_4$ ($y=0.1, 0.3, 0.5, 0.7$ and 0.9) were prepared using the standard ceramic method by mixing AR grade NiO , ZnO and Fe_2O_3 in the required mole proportions. A small amount of Bi_2O_3 (0.005 wt.%) was added as fluxing component. The suitable proportions of these oxides were taken and dry ground into fine powder. The resulting powder was mixed thoroughly in presence of distilled water to improve the homogeneity and then presintered at 900°C for 4 h in air. The mixture was milled again and the material was compressed to form pellets of 1.25 cm diameter and 0.27 cm thick by applying a pressure of 5 t/cm². The pellets were then sintered at 1250°C for 4 h in static air atmosphere. Finally, the samples were left to cool inside the electric furnace. The samples were investigated using X-ray diffraction analysis at room temperature with Philips PW 1390 X-ray diffractometer with cobalt (K_α) radiation and an iron filter. Infrared spectroscopic analysis, using KBr pellets was carried out using a FTIR 300E Fourier transform infrared spectrometer, Jasco (Japan). Determination of bulk density and apparent porosity of the prepared samples was carried out as described in the standard methods of testing materials. The percentage change in the diameter of samples before and after sintering was determined. The scanning electron microscope investigation

was carried out on a fresh fracture surface. The fracture surface was coated with thin film of evaporated gold, using an S 150 A sputter coater (England). Scanning electron micrographs were obtained using a JSM-T 20 scanning microscope, Jeol (Japan).

3. Results and discussion

The X-ray diffraction patterns of the prepared ferrite samples are shown in Fig. 1. The patterns show the reflection planes (111), (220), (311), (222), (400), (422), (511), (440) and (620) indicating the presence of the spinel of cubic structure. The patterns show also a slight shift in peaks position towards higher d -spacing values with increasing Zn content in the ferrite. The d -spacings

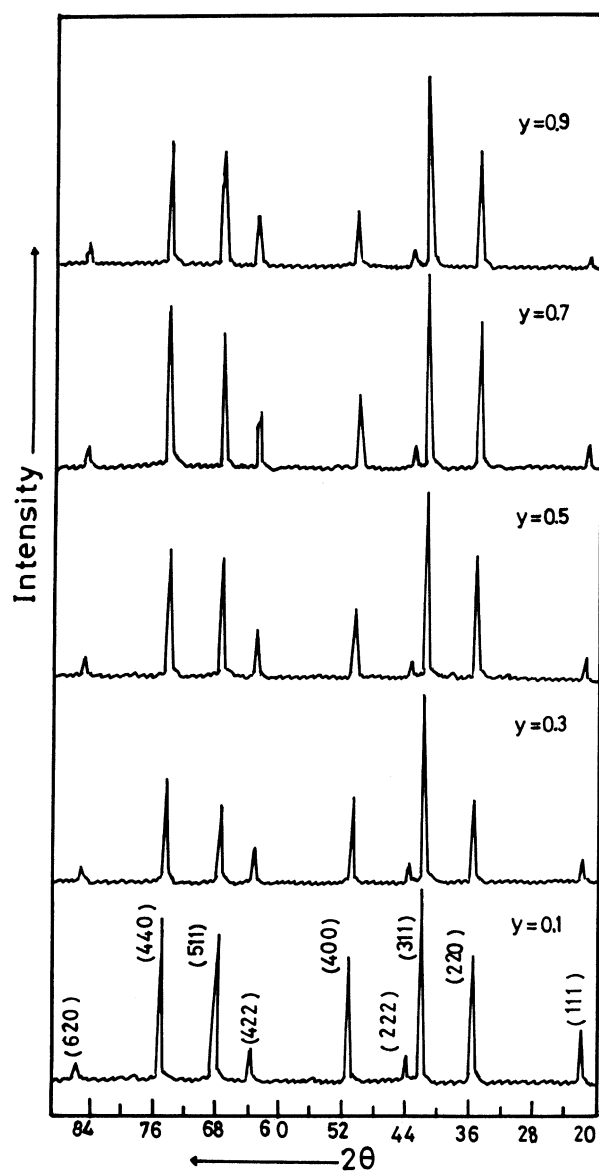
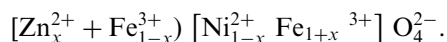


Fig. 1. X-ray diffraction patterns of $\text{Ni}_{1-y}\text{Zn}_y\text{Fe}_2\text{O}_4$, sintered at 1250°C .

for the recorded peaks were calculated according to Bragg's law. The values of the calculated lattice constant for different Zn concentrations are given in Fig. 2. The lattice constant is seen to increase linearly with Zn content for the composition $\text{Ni}_{1-y}\text{Zn}_y\text{Fe}_2\text{O}_4$ (Table 1). The Ni-Zn ferrite system has a cubic spinel configuration with unit cell consisting of eight formula units of the form



The Ni^{2+} ions have a marked preference for octahedral sites because of their favourable fit of charge distribution of this ion in the crystal field of the octahedral site. On other hand Zn^{2+} ions have preference for the tetrahedral site due to their readiness to form covalent bonds involving sp^3 hybrid orbitals [3]. The observed linear increasing of lattice constant with Zn content can be attributed to the large ionic radius of Zn^{2+} (0.84 \AA) as compared to the ionic radius of Ni^{2+} (0.74 \AA). A similar linear variation of lattice constant with Zn content has been observed by Joshi and Kulkarni [4] and Katakari et al. [5] for M-Zn ferrites with $\text{M} = \text{Ni}, \text{Co}, \text{Cu}, \text{Mg}$.

The room temperature IR spectra of the above-mentioned compositions are shown in Fig. 3. The spectra are recorded in the range from 200 cm^{-1} up to 1300 cm^{-1} . No absorption bands were observed above 1000 cm^{-1} . The spectra show two main absorption bands below 1000 cm^{-1} as a common feature of all the ferrites. The bands at 400 cm^{-1} and around 570 cm^{-1} are assigned as V_2 and V_1 , respectively. The band which appears at 240 cm^{-1} is assigned as V_3 . From IR spectra it is noticed that no shift occurs in position of bands at frequency V_3 and V_2 by increasing Zn content. Also, it can be seen that frequency V_1 is shifted to lower frequencies with increasing Zn ion concentration and consequently with

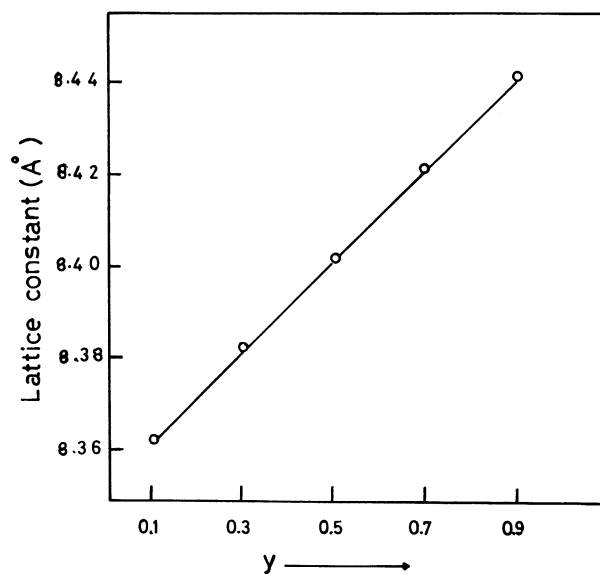


Fig. 2. Compositional variation of the lattice constant for $\text{Ni}_{1-y}\text{Zn}_y\text{Fe}_2\text{O}_4$.

Table 1
Data for $\text{Ni}_{1-y}\text{Zn}_y\text{Fe}_2\text{O}_4$, sintered at 1250 °C

y	Lattice constant (Å)	Position of the V_1 band (cm^{-1})	X-ray density (g/cm^3)	Bulk density (g/cm^3)	Apparent porosity (%)	Diameter shrinkage (%)
0.1	8.362	590	5.345	5.241	1.95	14.20
0.3	8.383	582	5.334	5.215	2.23	13.25
0.5	8.402	570	5.326	2.192	2.51	12.00
0.7	8.421	561	5.319	5.170	2.81	10.50
0.9	8.442	548	5.309	5.155	2.90	9.50

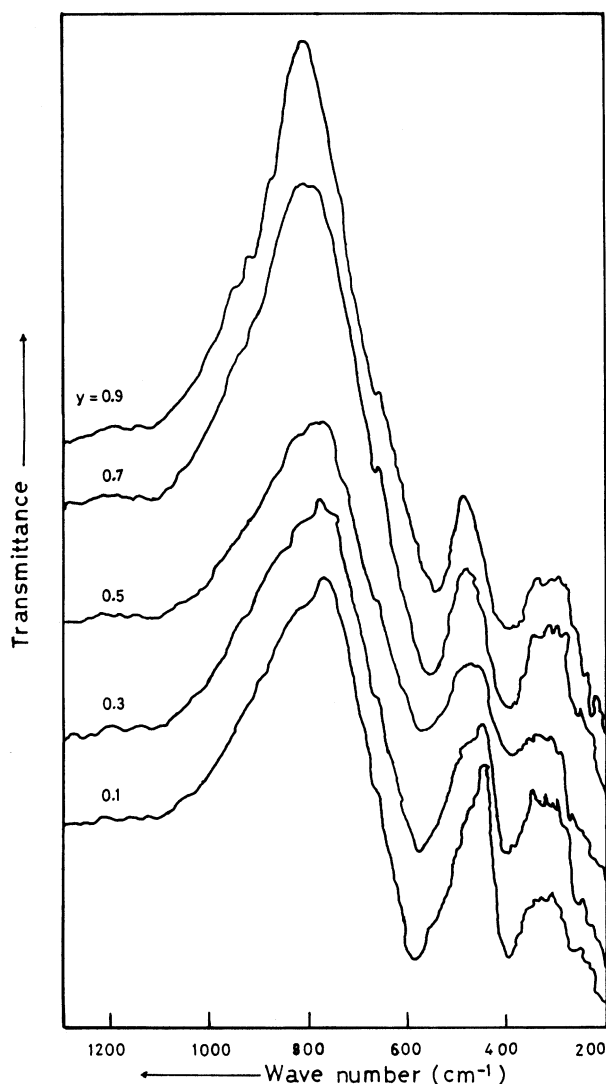


Fig. 3. IR absorption spectra of $\text{Ni}_{1-y}\text{Zn}_y\text{Fe}_2\text{O}_4$ sintered at 1250 °C.

decreasing Ni ion concentration. The high frequency band V_1 is in the range from 590 to 548 cm^{-1} (Table 1). The IR absorption bands of solids in the range between 100 and 1000 cm^{-1} are usually assigned to vibrations of ions in the crystal lattice [6]. According to Waldron [7] and Hafner [8] the ferrites can be considered as continuously bonded crystals. In ferrites the metal ions are situated in two different sub-lattices designated tetrahedral (A-site)

and octahedral (B-site) according to the geometrical configuration of the oxygen nearest neighbours. Waldron and Hafner, attributed the V_1 band to the intrinsic vibrations of the tetrahedral groups, the V_2 band to the octahedral groups and the V_3 band is associated with the vibration metal ions in the isotropic force fields of their octahedral or tetrahedral environments. According to Prakash and Bajjal [3] Zn^{2+} ions have preference for the tetrahedral sites replacing Fe^{3+} ions in Ni–Zn ferrites. The replacement of Fe^{3+} ions with Zn^{2+} ions having larger ionic radius and higher atomic weight at tetrahedral site in the ferrite lattice affects the $\text{Fe}^{3+}\text{--O}^{2-}$ stretching vibration. This may be a reason for the observed change in V_1 band positions. Fig. 3 also shows that, the IR absorption spectra of sample with Zn content ($y=0.7$) are more similar in the shape to that of sample with Zn content ($y=0.9$). The presence of isolated superparamagnetic clusters at B-sites screened by the diamagnetic Zn ions has been observed in Ni–Zn ferrites by Mössbauer studies [9,10]. A transition from a disordered to an ordered state has been confirmed at a certain temperature, which depends on the concentration of the diamagnetic ions [9,10]. According to [9], the disordered state in $\text{Ni}_{1-y}\text{Zn}_y\text{Fe}_2\text{O}_4$ with $y \leq 0.62$ is available at room temperature and according to Brabers and Vandenberghe [11], order-disorder phenomena in spinels have a great influence on the IR absorption spectra. The ordering on the B-sublattice reduces the space group and the number of IR active modes increases. Thus, a fine structure in the IR spectrum and from the close similarity between the IR spectra of $\text{Ni}_{0.3}\text{Zn}_{0.7}\text{Fe}_2\text{O}_4$ and $\text{Ni}_{0.1}\text{Zn}_{0.9}\text{Fe}_2\text{O}_4$, it might be concluded that the ionic order in both compounds is of the same kind at octahedral sites.

The variation of bulk density with composition as well as X-ray density variation, are represented in Fig. 4a. The X-ray density for each composition was calculated according to the relation $d_x = ZM/Na^3$ [12], where Z is the number of molecules per unit cell ($Z=8$), M the molecular weight, N Avogadro's number, and a^3 value of the unit cell volume. The bulk densities of the specimens were about 97–98% of the corresponding X-ray densities (Table 1). It is clearly shown that both densities decrease with increasing of Zn content, i.e. the bulk density nearly reflects the same general behavior of the

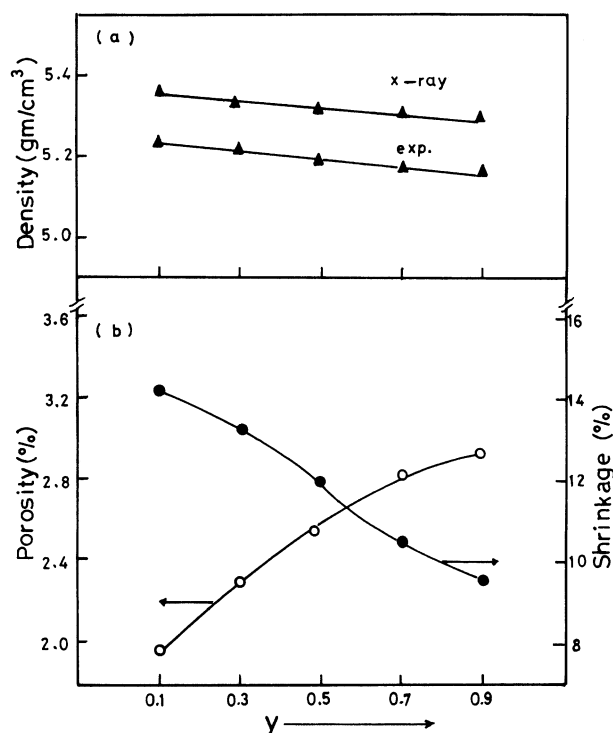


Fig. 4. Dependence of (a) X-ray and bulk density and (b) apparent porosity and diameter shrinkage, on Zn content in $\text{Ni}_{1-y}\text{Zn}_y\text{Fe}_2\text{O}_4$.

theoretical density. The smaller particle size or externally applied pressure increases the ratio of the densification rate to the reaction rate [13]. The densification rate at any temperature increases roughly with the heating rate for the case of extreme grain growth [14]. The powder particle size and applied pressure coupled with knowledge of the appropriate phase relations, would constitute a promising approach to the formation of material with the required high density and controlled microstructures [15]. The addition of Bi_2O_3 as a fluxing component permits to avoid loss of oxygen during sintering resulting in improved densification and homogenization of the sintered material [16]. Secrist and Turk [17] concluded that Ni–Zn ferrite samples sintered at sintering temperature $> 1170^\circ\text{C}$ showed rapid densification. From Fig. 4a, a difference is seen between values of d_x and d_{exp} , the difference between both data may be attributed to the porosity of the prepared samples. The observed decrease in bulk density with increasing Zn content in the ferrites can be ascribed to the difference in specific gravity of the ferrite components since NiO ($6.72 \text{ g}/\text{cm}^3$) is heavier than ZnO ($5.60 \text{ g}/\text{cm}^3$) [18]. The present results of apparent porosity and diameter shrinkage are shown in Fig. 4b. These data reveal clearly that, with increasing Zn concentration in the ferrite, apparent porosity of the

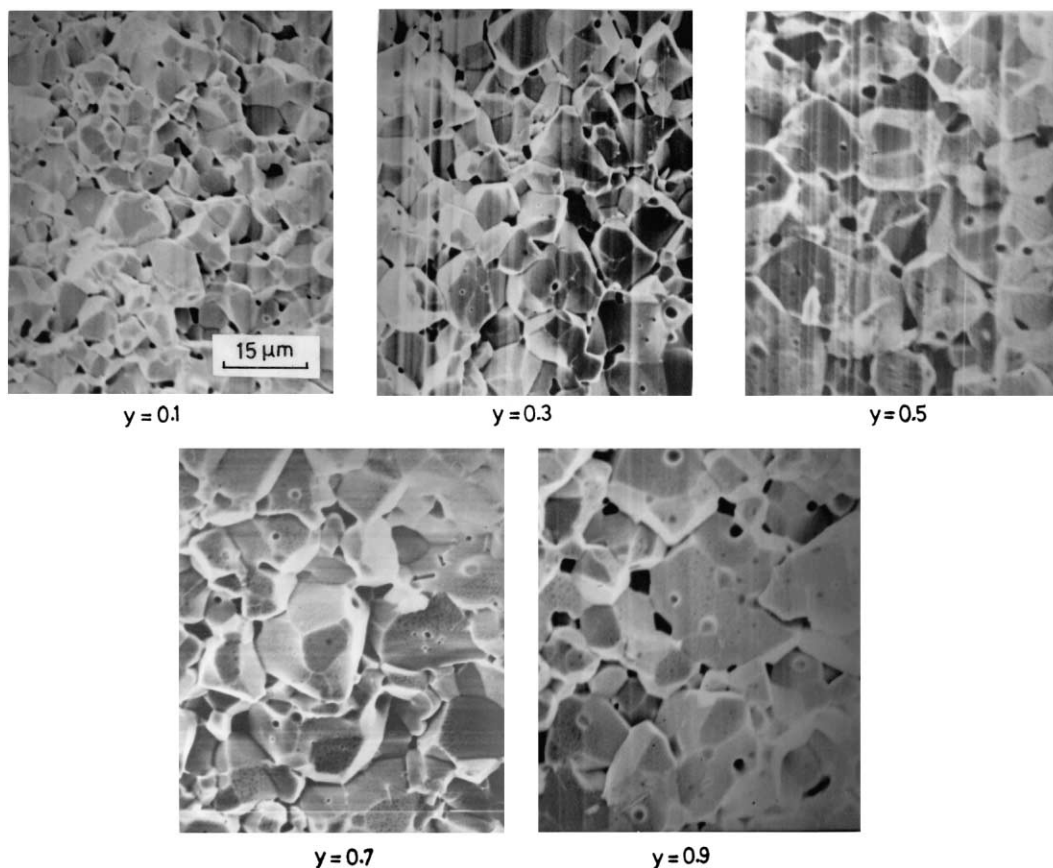


Fig. 5. Scanning electron micrographs of $\text{Ni}_{1-y}\text{Zn}_y\text{Fe}_2\text{O}_4$.

prepared samples increased meanwhile its diameter shrinkage was observed to decrease (Table 1). Also, from Fig. 4 we can easily see that, with increasing Zn content both bulk density and % shrinkage decrease, i.e. they have the same trend in behaviour.

Results of scanning electron microscope (SEM) studies on the prepared samples are shown in Fig. 5. The results show that, with increasing Zn content the grain size increased and the ferrite samples exhibit an exaggerated continuous grain growth with grains containing some fine pores.

4. Conclusions

The essential points established in the course of this study can be summarized as follows:

1. X-ray analysis data indicated that the increasing of Zn concentration in Ni–Zn ferrites, sintered at 1250 °C in static air atmosphere, gives ferrites having spinel cubic structure with increasing unit cell volume.
2. The IR absorption spectra at room temperature of the investigated samples showed an ionic ordered state at B-sites in $\text{Ni}_{1-y}\text{Zn}_y\text{Fe}_2\text{O}_4$ with $y \geq 0.7$.
3. The increasing Zn concentration in Ni–Zn ferrites leads to decrease in both bulk density and % diameter shrinkage and given ferrites having exaggerated grain growth with fine pores inside the grains.

References

- [1] H. Igarashi, K. Okazaki, Effects of porosity and grain size on the magnetic properties of NiZn ferrite, *J. Am. Ceram. Soc.* 60 (1977) 51–54.
- [2] D. Vladikova, L. Ilkov, S. Karbanov, Influence of the micro-structure on some microwave properties of substituted nickel ferrites, *Phys. Stat. Sol. (a)* 111 (1989) 145–154.
- [3] C. Prakash, J.S. Bajjal, Mossbauer studies on hyperfine field measurement in titanium doped nickel–zinc ferrites, *Solid State Commun.* 50 (1984) 557–559.
- [4] H.H. Joshi, R.G. Kulkarni, Susceptibility, magnetization and mossbauer studies of the magnesium zinc ferrite system, *J. Mater. Sci.* 21 (1986) 2138–2142.
- [5] S.V. Kakatkar, S.S. Kakatkar, R.S. Patil, A.M. Sankpal, S.S. Suryavanshi, D.N. Bhosale, S.R. Sawant, X-ray and bulk magnetic properties of the Ni–Zn ferrite system, *Phys. Stat. Sol. (b)* 198 (1996) 853–860.
- [6] V.A.M. Brabers, Infrared spectra of cubic and tetragonal manganese ferrites, *Phys. Stat. Sol.* 33 (1969) 563–572.
- [7] R.D. Waldron, Infrared spectra of ferrites, *Phys. Rev.* 99 (1955) 1727–1735.
- [8] S. Hafner, The absorption of some metal oxides with spinel structure, *Z. Krist.* 115 (1961) 331–358.
- [9] N.L. Pakhomova, V.N. Belogurov, V.A. Bylinkin, A.M. Vinnik, L.M. Kassimenko, P.E. Senkov, Low temperature transitions and spin configurations in nickel–zinc ferrite spinels, *Soviet Phys. Solid State* 19 (1977) 1060–1064.
- [10] R.K. Puri, U. Varshney, Mossbauer study of zinc (2+) and tin (4+) additives in nickel ferrites, *J. Phys. Chem. Solids* 44 (1983) 655–661.
- [11] V.A.M. Brabers, R.E. Vandenberghe, Ionic order and cation valencies in the spinels $\text{Cu}_{1.5}\text{Mn}_{1.5}\text{O}_4$ and CuGaMnO_4 , *Phys. Lett.* 44A (1973) 493–494.
- [12] M.A. Ahmed, Electrical properties of Co–Zn ferrites, *Phys. Stat. Sol. (a)* 111 (1989) 567–572.
- [13] Y. Shen, R.J. Brook, Preparation of zirconia-toughened ceramics by reaction sintering, *Sci. Sintering* 17 (1985) 35–47.
- [14] M.Y. Chu, M.N. Rahaman, L.C. De Jonghe, R.J. Brook, Effect of heating rate on sintering and coarsening, *J. Am. Ceram. Soc.* 74 (1991) 1217–1225.
- [15] M.N. Rahaman, L.C. De Jonghe, Effect of green density on densification and creep during sintering, *J. Am. Ceram. Soc.* 74 (1991) 514–519.
- [16] N.K. Gill, R.K. Puri, Mossbauer study of $\text{Li}_{0.5}\text{Fe}_{2.5-x}\text{Cr}_x\text{O}_4$ ferrites, *Spectrochim. Acta.* 41A (1985) 1005–1008.
- [17] D.R. Secrist, H.L. Turk, Electrical properties of high density iron deficient nickel–zinc ferrites, *J. Am. Ceram. Soc.* 53 (1970) 683–686.
- [18] David R. Lide, *Handbook of Chemistry and Physics*, CRC Press, New York, 1995.